ELSEVIER

Surface Science 383 (1997) 162–172

surface science

The surface electronic structure of stoichiometric and defective LiF surfaces studied with MIES and UPS in combination with ab-initio calculations

D. Ochs [a], M. Brause [a], P. Stracke [a], S. Krischok [a], F. Wiegershaus [a], W. Maus-Friedrichs [a], V. Kempter [a,*], V.E. Puchin [b], A.L. Shluger [b]

[a] *Physikalisches Institut der Technischen Universität Clausthal, Leibnizstrasse 4, D-38678 Clausthal-Zellerfeld, Germany*
[b] *Institute of Chemical Physics, University of Latvia, Rainis Blvd. 19, Riga, LV-1586, Latvia*

Received 20 November 1996; accepted for publication 19 February 1997

Abstract

UPS (He I) and metastable impact electron spectroscopy (MIES) spectra of the LiF(100) single crystal surface and stoichiometric LiF films are presented. The spectra are interpreted on the basis of ab-initio electronic structure calculations. Defective surfaces, produced by electron dosing, were studied in the same manner. The MIES spectra reveal that the electron dosing produces metallic patches on the surface, but no uniform Li adlayer. The calculations show that the F-center contribution to the electron emission is very close in energy to that from the metallic patches; thus, the two contributions cannot be distinguished by the present experimental techniques. © 1997 Elsevier Science B.V.

Keywords: Ab initio quantum chemical methods and calculations; Alkali halides; Electron stimulated desorption; Insulating surfaces; Metastable impact electron spectroscopy; Photoelectron spectroscopy; Surface defects

1. Introduction

During recent years, the electron spectroscopic techniques MIES and UPS (He I) have been demonstrated to be useful in monitoring changes in the electronic properties of surfaces during the growth of insulating films on metallic or semiconducting substrates [1–6]. In this paper, the combination of MIES and UPS is applied for the first time to the study of the electronic properties of defects introduced systematically into surfaces (here LiF films) by electron bombardment. Information on the defects is obtained from a comparison of the electronic structure of "as prepared" and defective surfaces.

Experimental study of the electronic properties of insulator surfaces by electron spectroscopic techniques is often hampered by difficulties in cleaning as well as by charge-up effects caused by the emission of electrons from the surface [7]. In order to avoid most of these difficulties, the following strategy is applied in this paper. LiF(100) single-crystal surfaces serve as a reference; charge compensation is achieved by slow electrons. Most of the other studies have been carried out on insulating films on W(110), thin enough to avoid charge-up phenomena, but thick

* Corresponding author. Fax: +49 5323 723600; e-mail: kempter@physik.tu-clausthal.de

PII S0039-6028(97)00153-2

enough to display the electronic structure of the LiF(100) sample. In particular, these films are subjected to electron bombardment, whereby the resulting changes in the electronic properties are monitored with MIES/UPS.

As in our previous studies of MgO [5] and Al_2O_3 [8] surfaces, the interpretation of the MIES and UPS spectra is based on the relevant densities of states (DOS) at the surface and the near-surface region, respectively. These DOS were calculated by ab-initio band-structure methods for both ideal and defective LiF(100) surfaces, and are also presented in this paper.

2. Experimental

The apparatus used has been described in detail previously [2,4,6]; on this occasion the growth of LiF, NaCl and CsI films on W(110) was studied in some detail with MIES and UPS (He I). Briefly, the apparatus is equipped with a cold-cathode gas discharge source for the production of metastable He^* ($^3S/^1S$) ($E^* = 19.8/20.6$ eV) atoms with thermal kinetic energies and He I photons ($E^* = 21.2$ eV) as a source for UPS. The triplet-to-singlet ratio was measured by studying He^*–Ar binary collisions to be 7:1. Metastable and photon contributions within the beam are separated by means of a time-of-flight technique combined with a double-counter system allowing us to register MIES and UPS spectra simultaneously. The angle of incidence of the probe beams was 45°; electrons emitted in the direction normal to the surface were analyzed. The simultaneous collection of a MIES/UPS spectrum took about 1 min. MIES and UPS measurements were performed using a hemispherical analyzer (Leybold EA10) with an energy resolution of about 250 meV. The kinetic energies $E_{kin} = 21.2$ eV (UPS) and $E_{kin} = 19.8$ eV (MIES) displayed in the spectra correspond to electrons emitted from the Fermi level of the substrate. These are the largest possible energies of the electrons achieved in the experiments. The low-energy onset of the electron spectra directly reflects the surface work function, and therefore its variation with exposure gives the exposure dependence of the work function. In order to avoid charge-up of the surface during the MIES and UPS measurements on LiF(100) single crystals, a tungsten filament was heated near the investigated surface. A potential difference of 2 V between filament and target was applied. The apparatus is also equipped with the surface analytical tools XPS, LEED and AES.

The following procedure was applied in order to clean the surface of the LiF(100) single crystal: repeated heating–sputtering cycles were required in order to remove adsorbates such as carbon monoxide. The crystal holder was heated to about 1000 K, and Ar^+ ions (500 eV; 1 μA cm^{-2}), incident at 70° with respect to the surface normal, were employed for sputtering. The cleanliness of the crystal was checked with XPS as well as with MIES and UPS (He I).

The LiF films on W(110) were prepared as follows: LiF molecules were supplied to the clean W(110) substrate by thermal evaporation (1100 K) of LiF powder. The thickness of the film produced was estimated to be 2 nm on the basis of XPS measurements. At this thickness the electronic properties of the film, as judged from the MIES and UPS (He I) measurements, are virtually indistinguishable from those of the bulk LiF(100) surface (see Section 4.1).

3. Theory

3.1. Methods for the interpretation of MIES and UPS spectra

The interpretation of the MIES results is, as in Refs. [5,8], based on the model introduced by Niehaus et al. [9–11]. Briefly, only Auger de-excitation of the He^* 1s2s probe atom can take place when it approaches sufficiently close to the insulator surface. This is due to the fact that the He 2s level is in resonance with the band gap of the insulator; consequently the 2s electron cannot make a transition to the surface and no contribution of the Auger capture process, dominating MIES spectra from clean metals, can be found. In the Auger de-excitation process, a surface electron fills the He 1s hole while the He 2s electron is emitted carrying the excess energy. The transition

probability is proportional to the density of occupied states involved in the Auger de-excitation process. The electron is emitted from the 2s state located at the He probe atom. Therefore, other than in UPS, the density of the empty states in the conduction band is of no concern for the interpretation of the MIES spectra. Within the model of Niehaus et al. [9–11] we find, as in previous work on oxides [5,8], that the surface DOS of the valence-band states are well represented by the MIES spectra.

Despite the fact that the UPS (He I) spectra depend on the joint density of filled and empty states in the near-surface region, we compare the DOS of the filled valence band directly with UPS (He I) spectra. This appears to be justified as long as we are mainly interested in the global features, such as the general shape, the total width and position of the valence-band spectrum.

3.2. Surface density of states

The density of states has been calculated using the CRYSTAL computer code [12,13] designed for ab-initio Hartree–Fock band-structure calculations on periodic systems. This method has been used previously to study the bulk properties of the LiF crystal and the ideal (100) surface of LiF [14]. However, up to now not much attention has been paid to calculation of the surface density of states, which is relevant to the surface-sensitive electron spectroscopic methods such as MIES. In the present study we concentrate on the modifications of the density of states induced by the atomic relaxation and by the presence of steps and kinks at the (100) surface. The basis set of atomic orbitals for Li and F ions, the lattice constant ($a_0 = 2.008$ Å) and other computational parameters of the method are taken from Ref. [14].

Besides the flat (100) surface, we have also calculated the band structure of the stepped (210) surface. It has steps of a height a_0 separated by flat (100) terraces of a width $2a_0$. Surface kinks have been simulated using the (111) (2×2)-reconstructed surface (see Fig. 1). This surface consists of (100), (010) and (001) facets of area of $4a_0^2$. It has a hexagonal symmetry and contains one F^- ion per unit cell in the top surface layer, which is coordinated by three Li^+ ions in the second layer. The subsequent layers contain either four F^- or four Li^+ ions. Thus, a zero surface dipole moment is maintained, making the surface stable. The density of states projected to the atoms in the middle layer of the slab converges to that found in the bulk calculation with an increasing number of layers. In order to satisfy this criterion, a thickness of five atomic layers was chosen for the (100) slab, nine layers for (210) and 13 for (111).

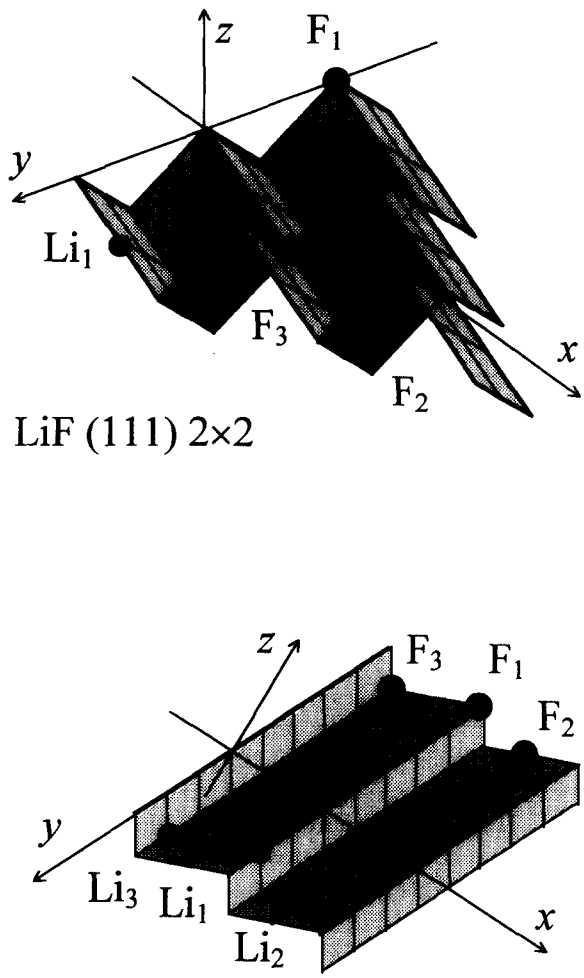

Fig. 1. LiF (210) and (111) (2×2) surfaces which have been used to simulate steps and kinks on the LiF surface.

The relaxation of the atoms in the top surface layer has been calculated for all three slabs. The minimum of the total energy of the slab with respect to the ion displacements has been found by the least-square fitting of the quadratic form to a sufficiently large number of calculated points. The optimized values of independent coordinates are listed in Table 1. The surface formation energy is defined as the difference between the Hartree–Fock total energy per unit cell of the relaxed slab (E_{slab}) and bulk crystal (E_{bulk}) divided by two, because the slabs have two equivalent surfaces

$$E_{surf} = (E_{slab} - nE_{bulk})/2,$$

where n is the number of LiF molecular units in the elementary unit cell of the slab. The relaxation energy is calculated as the difference in the surface energies of the relaxed and non-relaxed slabs. The relaxation energy of the most stable LiF(100) surface is very small, and the displacements of the surface ions with respect to their perfect lattice sites are less than 1% of the lattice spacing, in agreement with previous work [14]. The (210) and (111) surfaces are less stable than the (100) surface. The relaxation energy and the displacements of ions from their perfect lattice sites are much larger at these surfaces. The surface energy tends to increase with the density of surface steps and kinks. The displacements of the surface decrease the surface roughness: the ions sitting at the step, edge or at a kink site (for example F_1 in Fig. 1) move inwards, while those situated in the surface corners (such as F_3) move outwards.

In order to compare experimental electron spectra with the calculated density of states, broadening of the spectra due to different physical effects must be accounted for. In the case of LiF, having a relatively narrow valence band and large band gaps, the theory of the UPS core-line broadening can also be applied to the valence-band electron spectra. The core lines have a Gaussian shape due to phonon broadening effects. The lifetime broadening, which has a characteristic Lorentzian shape, is negligible. Therefore we make a convolution of the calculated DOS with a Gaussian function. The Gaussian width at half maximum depends on the hole relaxation energy and optical phonon frequency, as described in Refs. [15,16]. We found that a value of 1.0 eV (FWHM) gives the best agreement between the UPS F 2p valence-band spectrum measured at high photon energy ($h\nu =$ 125 eV) [17,18] and the calculated bulk density of states. We assume that the same value can also be applied to the surface density of states used for the simulations of MIES spectra, despite the fact that the phonon frequencies and the hole relaxation energy at the surface may differ from those in the bulk.

The density of states in the F 2p valence band projected to the F ions situated in the bulk of the crystal, at the flat (100) surface and at the step, edge and kink sites are shown in Fig. 2. In the subsequent discussion we shall use for these projected DOS the notation "bulk", "surface", "step" and "kink DOS", respectively. Two peaks in the bulk DOS are found, separated by 1.9 eV. The valence-band width without phonon broadening is

Table 1
Structure and energetics of calculated LiF surfaces (see Fig. 1 for notations)

Surface	(100)	(210)		(111)-(2×2)	
Displacements of ions (Å)	z	z	x	z	x
F_1	0.015	−0.023	0.134	−0.231	
F_2		−0.046	−0.016	−0.089	0.069
F_3		0.101	−0.049	0.388	
Li_1	−0.013	−0.093	0.195	−0.124	−0.159
Li_2		−0.091	−0.008		
Li_3		0.168	0.004		
Relaxation energy (eV/a_0^2)	0.0011	0.0333		0.2806	
Surface energy (eV/a_0^2)	0.0924	0.1687		0.4818	

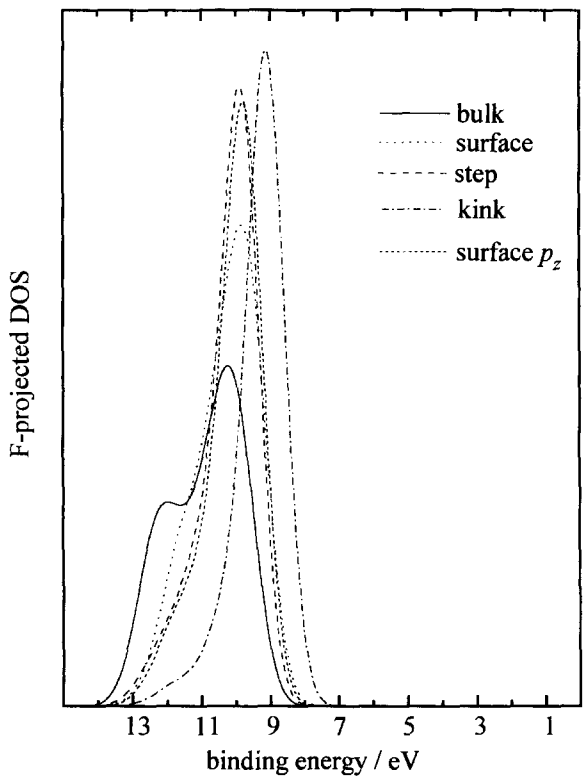

Fig. 2. The LiF bulk, surface, step and kink density of states. The curves show the DOS projected to the F atoms situated in the bulk of the crystal, in the top layer of the flat (100) surface, on the step edge at (210) surface and on the kink site at the faceted (2×2) (111) surface. Also shown is the F $2p_z$ projected DOS used for the simulation of the MIES spectrum.

3.7 eV. As mentioned above, the total width and the peak positions of the bulk DOS are in a good agreement with the results of Refs. [17,18] ($h\nu$ = 125 eV). At such a high energy, the contribution of the surface layers to the UPS intensity is negligible. At lower photon energy ($h\nu$ = 85 eV), the UPS spectrum has only one peak with the shoulder towards the higher electron binding energy instead of the second peak [17,18], similar to the calculated surface DOS. However, the peak of the p_z component of the surface DOS (the z axis is normal to the surface) is more symmetrical and sharper. The step DOS is apparently very close to the surface DOS, which makes the steps on the LiF(100) surface virtually invisible in UPS and MIES spectra. On the other hand, the peak of the kink DOS is split from the bulk and surface DOS.

3.3. Point defects

Electron bombardment of an alkali-halide crystal results in the formation of Frenkel pairs of defects in the anion sublattice (F–H pairs) [19,20]. The H centers (interstitial F atoms) are known to be unstable at the surface and decay with atom emission. At large electron doses and temperatures above the F-center mobility threshold, the F centers tend to agglomerate and form metal colloids. Therefore, for the discussion of the results obtained for the electron-dosed surface, the electronic structure of the F center and F_n agglomerates (n = 2–13) was simulated using the embedded molecular cluster method and the GAUSSIAN94 computer code [21]. The quantum cluster of cubic shape and 3×3×3 size, containing 13 F and 14 Li ions, was embedded into the 9×9×9 cage of "frozen" ions. Li^+ ions surrounding the quantum cluster were represented by the standard atomic-core pseudopotentials in order to prevent artificial delocalization of the cluster wavefunction, whereas the bare Coulomb potential was used for the F^- ions. The standard 6-31G basis set was used for Li and F in the cluster. The F centers and their agglomerates were produced by removing one or several F atoms from the cluster together with the core portion of its basis set (six s-type Gaussians) and the innermost sp Gaussian orbital from the valence basis. Three other sp-type Gaussians were split and left in the vacancy as floating orbitals in order to describe the wavefunction of the electron remaining in the vacancy.

The position of the F-center electron level with respect to the top of the valence band of the perfect crystal can be estimated with Koopmans' theorem as the difference between the corresponding one-electron energies. This simple procedure gives a value of 10.4 eV for the position of the F-center level relative to the top of the valence band. The binding energy of the electron at the highest occupied orbital of the F_n center or at the top of the valence band can be obtained more precisely using the ΔSCF method, i.e. by subtracting the energies of ionized and neutral states of corresponding clusters with or without defects. However, the absolute value of the binding energy calculated in this manner also contains an error

due to the incomplete account of the polarization of the lattice in our cluster model. We found the lowest binding energies to be 12.7 and 4.8 eV for the perfect cluster and that containing the F center, respectively. In order to avoid this systematic error, we calculate the differences between the F_n center and valence-band electron binding energies. The energy of the F-center electron relative to the top of the valence band was found to be 7.9 eV, which is smaller by 2.5 eV than the estimate based on the one-electron energy difference. Fig. 3 shows the one-electron energy spectra for the perfect cluster and those containing 1–13 F centers. These data provide only a qualitative picture for the development of the F_n agglomerate or Li colloid bands under the ionizing radiation because the electronic relaxation and polarization of the lattice in the ionized state of the crystal and the electron correlation effects are neglected. In order to make a quantitative comparison with experiment, we assume that the above-mentioned effects would introduce systematic corrections to the electron binding energies, and the error estimate of 2.5 eV obtained for the F center is also valid for the F_n centers. This correction has been taken into account in the comparison of the results in Fig. 3 with the experimental results.

The agglomeration of the F centers leads to a splitting of the energy levels by up to 2 eV depending on the size n. This splitting may provide a rough estimate of the width of the Li colloid band resulting for large n. The mean average value of the F_n energy levels shifts to lower binding energies by about 1 eV with increasing n. This value is expected to converge to the middle of the Li metallic colloid band when all F atoms are removed from the lattice. We should note that the present calculations neglect the effect of atomic relaxation. This approximation is well justified for the single F center, where the displacements of the surrounding ions are known to be negligible. For the larger F-center agglomerates, the displacements of Li atoms may become significant, because the arrangement of Li^+ ions in the LiF crystal is different from the crystalline structure of metallic Li. The distance between the nearest-neighbor Li atoms in the metal is larger by 7% than that in LiF. Therefore, we expect that the splitting between the F_n-center levels gives the upper estimate for the Li colloid band width.

The calculations give the DOS of the respective surface system, but not its absolute value on the energy scale. Therefore, theoretical spectra are shifted on the energy scale to obtain the best comparison with experimental spectra.

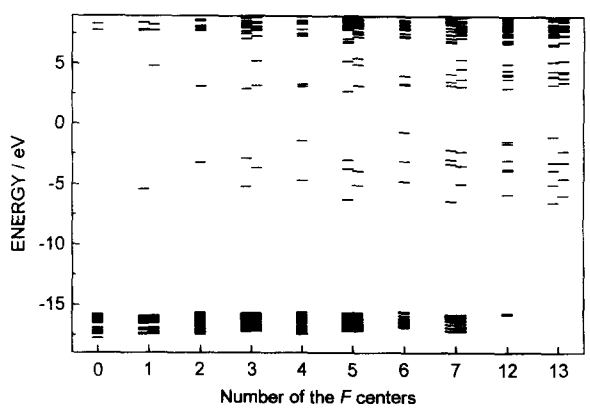

Fig. 3. One-electron energy spectrum (Hartree–Fock eigenvalues) of the F_n centers. Two sets of levels are shown in the cases with the open shell. A ΔSCF correction has been added to the one-electron energies.

4. Experimental results and discussion

4.1. Undamaged ("as prepared") surfaces of LiF(100) single crystals and LiF films on W(110)

The UPS (He I) and MIES spectra of the LiF(100) single crystal are presented in Fig. 4. All binding energies refer to the Fermi level E_F, which was determined with a metal target at the position of the insulator target. The UPS (He I) and MIES results show several common characteristics: both display valence-band emission with a pronounced maximum at around 9.5 eV. The top of the valence band is found at about 8.0 eV below E_F. The valence-band structure is wider in the UPS (He I) spectrum (3 eV as compared to 2 eV FWHM in MIES). The UPS (He I) spectra show some asymmetry in the valence-band emission towards larger binding energies, but no indication for the second peak at about 2 eV higher binding energies (as compared to the main maximum). This additional

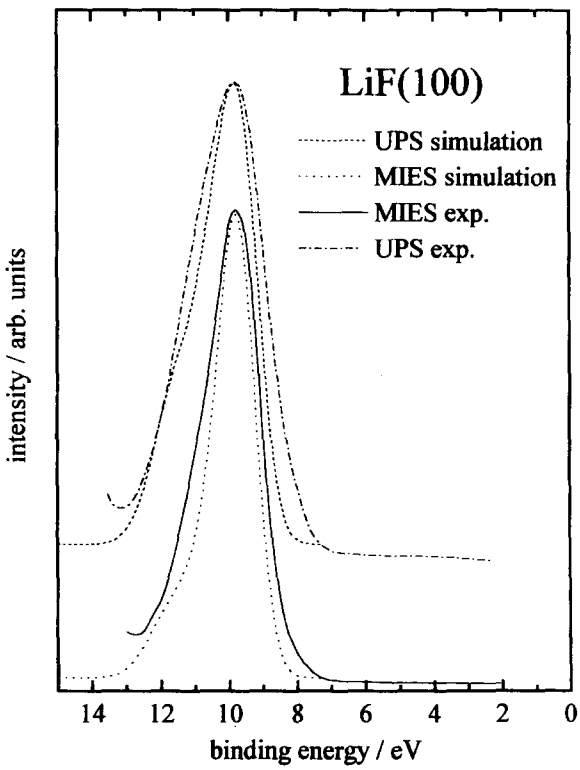

Fig. 4. Comparison of experimental and simulated MIES and UPS spectra of the LiF(100) surface. Simulated spectra utilize the F $2p_z$ projected surface DOS (MIES) and the full surface DOS (UPS) of Fig. 2.

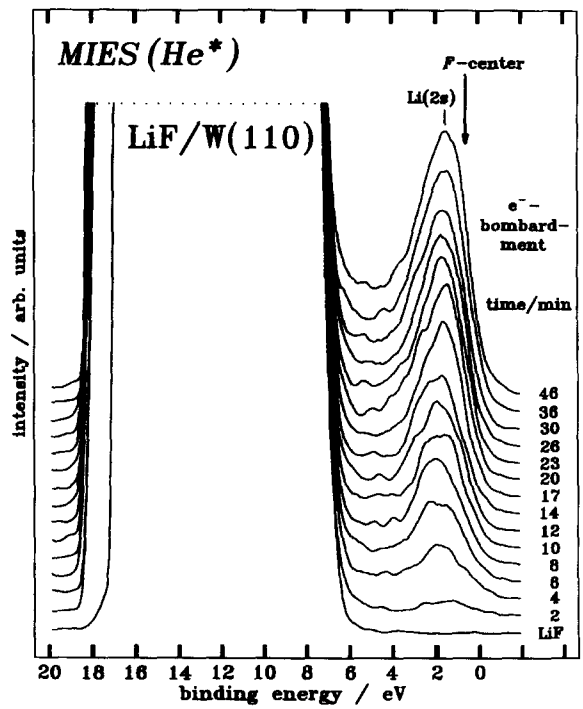

Fig. 5. MIES spectra of a LiF film on W(110) as a function of the electron dosing time. The bottom spectrum is for the stoichiometric LiF film (2 nm thickness). The arrow denotes the calculated binding energy of the F center.

peak was observed for MgO and Al_2O_3 [5,8] at $h\nu = 21.2$ eV. Beyond $E_B \approx 13$ eV, the MIES and UPS spectra are dominated by slow electrons from inelastic electron–electron interaction and from the tungsten filament applied for charge compensation. Therefore the experimental spectra are cut off at this value.

MIES and UPS data were also obtained from 2 nm thick LiF films on W(110) produced by the procedure described in Section 2. They are very similar to those shown in Fig. 4, with the main difference being that less intensity is visible in the lower part of the band-gap between $E_B = 0$ and 6 eV (see also the bottom spectrum in Fig. 5). The intensity seen above the top of the valence band may, apart from phonon broadening, reflect the contribution from surface irregularities produced during the preparation of the crystal and the film (see Section 4.3). On the other hand, the comparison between LiF(100) and LiF/W(110) indicates that the procedure for cleaning LiF(100), as described in Section 2, does not produce F-center related point defects (see also Section 4.2). For LiF/W(110) we have determined the surface work function from the low-energy cut-off in the measured spectra. The sum of the work function (3 eV) and the valence-band offset (as measured from E_F) (8 eV) gives 11.0 eV for the valence-band offset from the vacuum level.

In the following we interpret the UPS (He I) and MIES spectra by comparing them with earlier data and with the results of Fig. 2. The UPS (He I) data of Fig. 4 are in general agreement with our earlier data presented in Ref. [4] as well as with those of Refs. [17,18] as far as the width of the valence band and the position of the top of the valence band with respect to the vacuum level are concerned. The best agreement with simulation is obtained when utilizing the full surface DOS (curve "surface" of Fig. 2) for comparison (included in

Fig. 4). For the comparison with experiment, the simulated spectrum is shifted in such a manner that the maxima coincide. MIES data for LiF films on W(110) were reported previously in Refs. [3,4]: in Ref. [3] the growth of LiF adlayers was studied starting from the modification of the electronic structure of the substrate DOS by single adsorbed LiF molecules up to the emergence of the electronic structure of the LiF bulk. The MIES spectra could be synthesized with the model introduced in Refs. [9–11] and making plausible assumptions concerning the electronic structure of the surface modified by LiF adsorption. In Ref. [22] the surface DOS required for the simulation of ion impact electron spectroscopy (IIES) spectra (induced by slow He^+ and He^{2+} ions) was derived from experimental MIES results for LiF films on W(110). The extracted surface DOS agreed well with that from ab initio calculations for the LiF bulk [14]. Our present results for LiF/W(110) and LiF(100) agree well with these previous results. The theoretical MIES spectrum shown in Fig. 4 utilizes the DOS projected to the surface F $2p_z$ orbital (see Fig. 2). Again, the simulated spectrum is shifted in such a manner that the maxima coincide. The simulation predicts correctly that the MIES spectra are narrower than the UPS spectra. This suggests strongly that the MIES results are dominated by the emission of electrons from those states which protrude furthest into the vacuum (i.e. the F $2p_z$ orbitals), while the UPS spectra are sensitive to the full F 2p DOS in the near-surface region.

4.2. Electron-dosed LiF films on W(110)

The MIES data obtained during the dosing of an ~ 2 nm thick LiF film on W(110) with electrons (1.4 keV, 6×10^{12} electrons $mm^{-2} s^{-1}$) are presented in Fig. 5. The spectra are magnified in such a way that the peak just below E_F becomes visible. The main spectral maximum at $E_B = 9.5$ eV is larger by a factor of 10^3. No emission above the top of the valence-band maximum (apart from an extremely weak monotonous tail) is visible for the undosed layer. A structure just below E_F (zero energy), denoted "Li(2s)", develops during the dosing; it is centered about 5 eV above the top of the valence band. On the other hand, UPS (He I) spectra (not shown here) taken simultaneously with the MIES spectra only display the valence-band emission; Li 2s is not seen in the UPS spectra.

The origin of Li(2s) has been established in the following way: a feature similar in shape and position occurs when clean W(110) is exposed to Li atoms [4]. More generally, such a feature near E_F is always seen with MIES when a metal or semiconductor surface is exposed to alkali atoms as soon as the adlayer develops metallic properties and the work function becomes sufficiently low (typically below 2.5 eV). The simulation of the MIES spectra obtained under these conditions confirmed that Li(2s) arises mainly from the autodetachment of He^{-*} temporary ions formed by the resonant transfer of a surface electron to the probe atom. This occurs at around 0.6 ML in terms of the saturation coverage at room temperature. On the basis of these findings, we draw the following conclusion: at least for larger doses (of the order of 10^{16} electrons cm^{-2} or more) the structure Li(2s) emerging during the electron dosing of the LiF film is due to the transfer of a surface electron to the metastable probe atom from metallic patches at the surface. This leads to the formation of $He^{-*}(^2S)$, followed by autodetachment of the temporary ion. For such doses the partial metallization of the defective surface appears to be well established [23,24]. We find, however, that the valence-band emission is attenuated by 20% at most during dosing. This shows that no uniform adlayer has developed. Instead, metallic clusters or colloids are formed (see Refs. [23,24]).

It is generally accepted that the formation of areas with metallic character is preceded by the production of the F centers and their aggregates (Ref. [25], and references therein). In principle, MIES appears to be suited to detect these defect types via the Auger de-excitation process involving the F-center electron. However, the calculated position for the emission from the ionization of the F centers and their agglomerates (see Section 3.3) more or less coincides with that of the peak from the autoionization of He^{-*} formed at metallic areas on the defective surface (see Figs. 3 and 5). Thus, it is not straightforward to distinguish with MIES between the presence of F cen-

ters, their agglomerates and metallic clusters at the defective LiF surface. Our observations are compatible with the following scenario: the lowest dose at which the feature Li(2s) is visible is about 10^{15} electrons cm^{-2}. Nevertheless, it appears to be sufficiently large to create of the order of 10^{15} F centers in a film of 2 nm thickness [26]. These F centers are mobile at room temperature and will neutralize Li^+ ions at the surface. This leads ultimately to the formation of Li clusters with metallic character at the film surface even at the lowest applied doses. Summarizing, the results of Fig. 5 document the transformation of the initially stoichiometric surface into one with patches of metallic character.

4.3. *LiF films annealed after electron dosing*

Fig. 6 shows the development with target temperature of the intensity seen in the band gap.

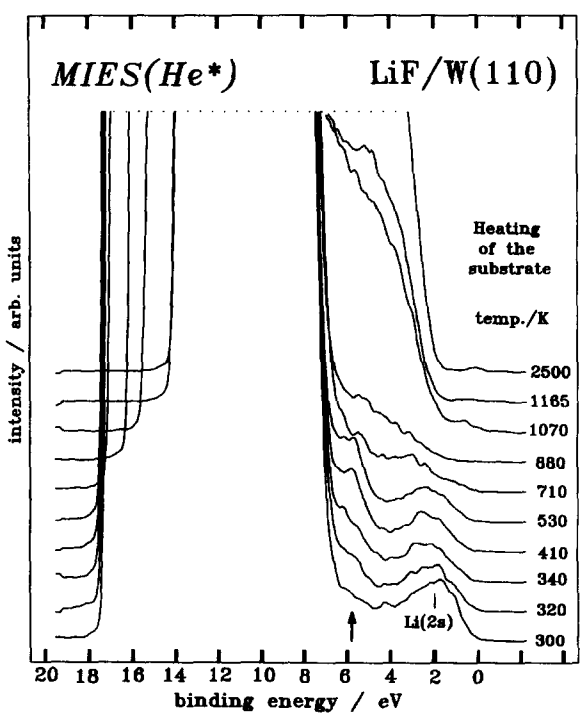

Fig. 6. MIES spectra obtained during the stepwise heating of the defective surface represented by the top spectrum shown in Fig. 5. The arrow shows the top of the valence band calculated for the (111) surface.

Initially the emission labeled "Li(2s)" comes from the metallic regions of the damaged surface (see Section 4.2). Above 340 K a peak ($E_B = 5.5$ eV with respect to E_F) develops which increases in intensity up to about 530 K. We attribute this feature to the oxygenation of the metallic regions by background molecules, in particular CO_2 and CO. This interpretation is based on the following facts: (i) we have observed a very similar structure during the oxygenation of Li adlayers on tungsten [27], and (ii) Jardin et al. [28] have concluded on the basis of AES and EELS measurements that Li atoms present on top of a damaged LiF surface are oxidized in the ambient vacuum. On the basis of the EELS data, the oxide was attributed to Li_2O. Li(2s) disappears between 530 and 710 K, together with the intensity attributed to Li–O complexes. However, some emission remains visible above the top of the valence band when Li(2s) has disappeared (see below). Increasing the temperature further, the LiF film is removed completely (above about 1070 K). The removal of the film is also signaled by the strong rise of the surface work function in this temperature range (see shift of the low-energy onset of the spectra towards higher energies in Fig. 6). On the basis of the results obtained during the growth of a LiF film on tungsten [4], we identify the emission at these temperatures as being due to the Auger capture process involving two electrons from the conduction band of the tungsten substrate.

In the following we discuss the origin of the emission seen between 710 and 1070 K on the basis of the results of Fig. 2: because this emission was not present before electron dosing, it must be ascribed to damaged areas of the surface with low-coordinated fluorine species such as those located at edge sites (see below). The results of Fig. 3 show that the emission is not due to the ionization of the F_n centers ($n = 1$–13). It was demonstrated for MgO [29] that emission at these energies arises from the ionization of low-coordinated anions.

The calculated position of the peak of the kink DOS, at 1 eV lower binding energy relative to the main maximum of the valence-band emission, is indicated by the arrow in Fig. 6. The tails in the experimental spectra extend to even lower binding energies. We should note, however, that other

possible configurations of the low-coordinated fluorine may have a different splitting of the level from the top of the valence band than the splitting we have calculated. Thus, we suggest that the observed tails are caused by the microroughness of the damaged surface. This roughness can be visualized in the following way: as stated above, the metallization is caused by F-center diffusion to the surface. This leads to the aggregation of the vacancies in the anion sublattice. After removing the metallic areas (see spectra between 700 and 1050 K), the damaged areas with low-coordinated F ions become accessible to ionization in the Auger de-excitation process. Part of the weak tails seen in particular for the LiF(100) surface may also have to be attributed to the microroughness. However, this contribution is superimposed by that arising from the phonon broadening of the valence-band emission.

5. Summary

The electronic structure of LiF surfaces, films on W(110) and LiF(100) single-crystal surfaces, is studied with the electron spectroscopic techniques metastable impact electron spectroscopy (MIES) and UPS (He I). The change of the electronic structure during electron dosing of the surfaces is monitored with the same techniques. An interpretation of the results is made on the basis of ab initio electronic structure calculations for both the stoichiometric and the defective surface. Two types of defects could be identified: (i) metallic patches induced by the dosing with electrons, and (ii) edge-type defects, already present on the stoichiometric LiF(100) surface but much more pronounced on the damaged surface. The task of detecting F centers and their agglomerates at LiF surfaces with MIES is made virtually impossible by the fact that the structure from their ionization coincides with that caused by the metallic patches of the surface.

Acknowledgements

Financial support from the Deutsche Forschungsgemeinschaft is gratefully acknowledged (Ke 155/24 and 436 LET 113/1). The calculations were performed at the Regionales Rechenzentrum für Niedersachen (RRZN) in Hannover.

References

[1] H. Ishii, S. Masuda, Y. Harada, Surf. Sci. 239 (1990) 220.
[2] A. Hitzke, S. Pülm, H. Müller, R. Hausmann, J. Günster, S. Dieckhoff, W. Maus-Friedrichs, V. Kempter, Surf. Sci. 291 (1993) 67.
[3] S. Pülm, A. Hitzke, J. Günster, W. Maus-Friedrichs, V. Kempter, Surf. Sci. 325 (1995) 75.
[4] S. Pülm, A. Hitzke, J. Günster, H. Müller, V. Kempter, Radiat. Eff. Def. Sol. 128 (1994) 151.
[5] D. Ochs, W. Maus-Friedrichs, M. Brause, J. Günster, V. Kempter, V. Puchin, A. Shluger, L. Kantorovich, Surf. Sci. 365 (1996) 557.
[6] S. Dieckhoff, H. Müller, H. Brenten, W. Maus-Friedrichs, V. Kempter, Surf. Sci. 279 (1992) 233.
[7] V.E. Henrich, P.A. Cox, The Surface Science of Metal Oxides, Cambridge University Press, Cambridge, 1994.
[8] V.E. Puchin, J.D. Gale, A.L. Shluger, E.A. Kotomin, J. Günster, M. Brause, V. Kempter, Surf. Sci. 370 (1997) 190.
[9] P.A. Zeijlmans van Emmichhoven, P.A.A.F. Wouters, A. Niehaus, Surf. Sci. 195 (1988) 115.
[10] P. Eeken, J.M. Fluit, A. Niehaus, I. Urazgildin, Surf. Sci. 273 (1992) 160.
[11] H. Brenten, H. Müller, A. Niehaus, V. Kempter, Surf. Sci. 178 (1992) 183.
[12] R. Dovesi, C. Pisani, C. Roetti, M. Causá, V.R. Saunders, CRYSTAL-88, QCPE program No. 577, Bloomington, IN, 1989.
[13] C. Pisani, R. Dovesi, C. Roetti, Hartree–Fock Ab-initio Treatment of Crystalline Systems, Lecture Notes in Chemistry, Springer, Heidelberg, 1988.
[14] M. Causá, R. Dovesi, F. Ricca, Surf. Sci. 280 (1993) 1.
[15] M. Iwan, C. Kunz, Phys. Lett. A 60 (1977) 345.
[16] J.J. Mackham, Rev. Mod. Phys. 31 (1959) 956.
[17] D.A. Lapiano-Smith, E.A. Eklund, F.J. Himpsel, Appl. Phys. Lett. 59 (1991) 2174.
[18] F.J. Himpsel, L.J. Terminello, D.A. Lapiano-Smith, E.A. Eklund, J.J. Barton, Phys. Rev. Lett. 68 (1992) 3611.
[19] W. Hayes, A.M. Stoneham, Defects and Defect Processes in Nonmetallic Solids, Wiley, New York, 1985.
[20] K.S. Song, R.T. Williams, Self-Trapped Excitons, Springer, Berlin, 1993.
[21] M.J. Frisch, G.W. Trucks, M. Head-Gordon, P.M.W. Gill, M.W. Wong, J.B. Foresman, B.G. Johnson, H.B. Schlegel, M.A. Robb, E.S. Replogle, R. Gomperts, J.L. Andres, K. Raghavachari, J.S. Binkley, C. Gonzalez, R.L. Martin, D.J. Fox, D.J. Defrees, J. Baker, J.J.P. Stewart, J.A. Pople, GAUSSIAN92, Gaussian Inc., Pittsburgh, PA, 1992.

[22] F. Wiegershaus, S. Krischok, D. Ochs, W. Maus-Friedrichs, V. Kempter, Surf. Sci. 345 (1996) 91.
[23] Onn Dou, D.W. Lynch, A.J. Bevolo, Surf. Sci. 219 (1989) L623.
[24] N. Seifert, Hui Ye, D. Lin, R.G. Albridge, A.V. Barner, N. Tolk, W. Husinsky, G. Betz, Nucl. Instrum. Methods B 72 (1992) 401.
[25] M. Szymonski, in: Springer Series in Surface Science, vol. 19, DIET IV, Springer, Berlin, p. 270.
[26] C.A. Ordonez, D.P. Russel, M. Portillo, Surf. Sci. 290 (1993) 113.
[27] W. Maus-Friedrichs, S. Dieckhoff, M. Wehrhahn, S. Pülm, V. Kempter, Surf. Sci. 271 (1992) 113.
[28] C. Jardin, P. Durupt, J. Davenas, Radiat. Eff. Def. Sol. 137 (1995) 29.
[29] L.N. Kantorovich, J.M. Holender, M.J. Gillan, Surf. Sci 343 (1995) 221.